Analysis of the Substituent Effect on the Reactivity Modulation during Self-Protonation Processes in 2-Nitrophenols

6 AUTHORS, INCLUDING:

Ignacio Gonzalez
Metropolitan Autonomous University
280 PUBLICATIONS **3,484** CITATIONS

Analysis of the Substituent Effect on the Reactivity Modulation during Self-Protonation Processes in 2-Nitrophenols

Jimmy Alexander Morales-Morales,[†] **Carlos Frontana,***[,‡] **Martha Aguilar-Martínez,***[,†] **José Antonio Bautista-Martínez,**[†] **Felipe J. González,**[‡] **and Ignacio González**[£]

Facultad de Química, Universidad Nacional Autónoma de México, Ciudad Universitaria, C.P 04510, México, DF., México, Departamento de Química, Centro de Investigación y Estudios Avanzados-Zacatenco, Av. Instituto Politécnico Nacional No. 2508. Col. San Pedro Zacatenco, C. P. 07360. México, DF., México, and Departamento de Química, Universidad Autónoma Metropolitana-Iztapalapa, Apdo Postal 55-534, C.P 09340, México, DF., México
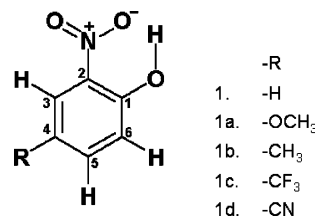
A voltammetric and spectroelectrochemical ESR study of the reduction processes of five substituted 4-R-2-nitrophenols (R = −H, −OCH$_3$, −CH$_3$, −CN, −CF$_3$) in acetonitrile was performed. In the potential range considered here (−0.2 to −2.5 V vs Fc$^+$/Fc), two reduction signals (I$_c$ and II$_c$) were detected; the first one was associated with the formation of the corresponding hydroxylamine via a self-protonation pathway. The voltammetric analysis at the first reduction signal showed that there are differences in the reduction pathway for each substituted 4-R-2-nitrophenol, being the $E_{1/2}$ values determined by the inductive effect of the substituent in the meta position with respect to the nitro group, while the electron-transfer kinetics was determined by the protonation rate (k_1^+) of the anion radical electrogenerated. However, at potential values near the first reduction peak, no ESR signal was recorded from stable radical species, indicating the instability of the radical species in solution. Nevertheless, an intense ESR spectrum generated at the second reduction peak was detected for all compounds, indicating the monoelectronic reduction of the corresponding deprotonated 4-R-2-nitrophenols. The spin-coupling hyperfine structures revealed differences in the chemical nature of the electrogenerated radical; meanwhile, the −CF$_3$ and −CN substituents induced the formation of a dianion radical structure, and the −H, −CH$_3$, and −OCH$_3$ substituents provoked the formation of an anion radical structure due to protonation by acetonitrile molecules of the initially electrogenerated dianion radical. This behavior was confirmed by analyzing the ESR spectra in deuterated acetonitrile and by performing quantum chemical calculations of the spin densities at each site of the electrogenerated anionic radicals.

Introduction

An important number of pharmacologically active compounds have a nitro aromatic group in their molecular structures.[1−6] Due to the ability of these drugs to be reduced at the nitro group, they are metabolized to the corresponding amines via the formation of nitroso and hydroxylamine derivatives. Nevertheless, it is known that biological activity of nitro compounds is not due to the final products of reduction but to the formation of intermediates, possibly free radicals.[7]

In the case of nitrophenols, their reduction mechanism was studied earlier in aprotic media, where it was found to be dependent on the acidity of the phenolic proton. The reduction mechanism of the nitro group in this type of compounds involves the presence of self-protonation processes.[8] This set of reactions provokes a destabilization of the first electrogenerated nitro anion radical (HO(ϕ-R)NO$_2$$^{•−}$), and therefore, the first reduction process proceeds as a multielectronic transfer. Due to this fact, it is apparently not possible to study the structural properties of the anion radical of 2-nitrophenol in acetonitrile solution.[9]

Figure 1. Structures of the 4-R-2-nitrophenol derivatives studied in this work.

An interesting alternative to stabilize the nitro anion radical is to change the acidity of the phenolic proton in a given nitrophenol derivative. In the case of substituted 2-nitrophenols, this can be achieved by modifying the chemical nature of a substituent group in the molecule, which can add or withdraw electronic density to the hydroxy moiety; the substituent effect changes the acidity of the molecule in a similar way as has been studied in α-OH quinones,[10,11] modifying the reduction pathway, which would be particularly important for stabilizing an anion radical structure.

Even though there has been a recent interest in studying the reactivity of nitro compounds,[12−14] the effect of the substituent on the electrochemical reactivity of such compounds is scarcely considered,[15] and the number of papers dealing with the influence of the chemical structure on the kinetic parameters of the electron-transfer process is also small.[16] Therefore, it is

* To whom correspondence should be addressed. E-mail: ultrabuho@yahoo.com.mx. Tel: + 52 55 50613800, Ext. 4001. Fax: + 52 55 50613389 (C.F.); E-mail: marthaa@servidor.unam.mx. Tel: + 52 55 56 22 37 58. Fax: + 52 55 56 22 37 58 (M.A.M.).
† Universidad Nacional Autónoma de México.
‡ Centro de Investigación y Estudios Avanzados-Zacatenco.
£ Universidad Autónoma Metropolitana-Iztapalapa.

of importance to analyze the electronic effects of a given substituent in order to gain more insight into the parameters which can determine the chemical reactivity of the nitro group, as many biologically active nitroaromatic compounds undergo self-protonation processes.[13]

In this work, the effect of the substituents in the reduction mechanism of 4-R-2-nitrophenols (Figure 1) was studied, employing cyclic voltammetry. The presence of radical species electrogenerated during the electrochemical study of these compounds was tested by performing spectroelectrochemical experiments using electron spin resonance (ESR).

Experimental Section

Techniques and Apparatus. Cyclic voltammetry experiments were performed using a PGSTAT 100 AUTOLAB electrochemical analyzer interfaced with a personal computer. Cyclic voltammetry experiments at several scan rates within the interval of $0.01 \leq \nu \leq 70$ V s^{-1} were performed, applying IR drop compensation with R_u values determined from positive feedback measurements ($R_u = 112$ Ohms).[17,18] This value was also independently determined as the real component of the measured impedance at high frequencies (about 10 kHz) from a Nyquist diagram, leading to a variation in the anodic peak potential of a 1 mM solution of ferrocene of 1 mV dec^{-1} (from 0.01 to 70 V s^{-1}) and of the cathodic peak potential for a 1 mM solution of anthracene of 1.5 mV dec^{-1}. A glassy carbon disk electrode (0.07 cm^2) was used as a working electrode, polished with 0.05 μm alumina (Buehler), and rinsed with acetone before each voltammetric run. A platinum wire and a commercial aqueous calomel electrode, this last being separated from the medium in a salt bridge filled with the supporting electrolyte solution, were used as the auxiliary and reference electrodes, respectively. The potential values obtained are referred to the ferrocenium/ferrocene (Fc$^+$/Fc) couple, as recommended by IUPAC.[19] The potential for this redox couple, determined by voltammetric studies, was 0.41 V versus the employed reference. The studies were carried out in an inert atmosphere by saturation with high-purity nitrogen (Praxair grade 5.0) at room temperature (approx. 22 °C).

Reagents. The following 4-R-2-nitrophenols derivatives (**1**: R = −H; **1a**: R = −OCH$_3$; **1b**: R = −CH$_3$; **1c**: R = −CF$_{3;}$ **1d**: R = −CN, Figure 1) were used (Aldrich A. R. grade). These compounds were further purified by sublimation and distillation according to their aggregation state. Acetonitrile (CH$_3$CN), Burdick and Jackson grade HPLC, distilled from P$_2$O$_5$ was used as the solvent. The 0.1 mol L^{-1} tetraethylammonium tetrafluoroborate (Et$_4$NBF$_4$, Fluka Chemika) solutions were prepared with the distilled solvent and used as the supporting electrolyte.

The 1 × 10^{-3} mol L^{-1} solutions of the studied 4-R-2-nitrophenols were prepared by dissolving the desired compound in a 0.1 mol L^{-1} Et$_4$NBF$_4$/CH$_3$CN solution. The solutions were purged with high-purity nitrogen (Praxair, Grade 5.0) for 45 min before each series of experiments. For the studies in deuterated acetonitrile (CD$_3$CN), 1 × 10^{-3} mol L^{-1} solutions of compounds **1** and **1a** were employed by dissolving the corresponding compound in a 0.1 mol L^{-1} Et$_4$NBF$_4$/CD$_3$CN (Aldrich 99% R. A. grade, stored with 3 Å Merck molecular sieves) solution.

Tetraethylammonium hydroxide, 1 mol L^{-1}, in water (Aldrich) was used to deprotonate the corresponding 4-R-2-nitrophenols by adding stoichiometric quantities to the solution under study. The tetraethylammonium salts of the corresponding 4-R-2-nitrophenols were previously prepared with equimolar quanti-

ties of 4-R-2-nitrophenols and 0.1 M tetraethylammonium hydroxide. The salts were obtained by vacuum drying of the reaction solution and were stored in the oven.

The pK_a values of the nitrophenols studied here were determined by potentiometric titration of 1 mM solutions in CH$_3$-CN using a CONDUCTRONIC pH meter model pH20 with a millivolt scale, employing a Ag/AgCl reference electrode (Radiometer, model REF361) filled with 0.1 M tetrabutylammonium chloride and a glass electrode as the selective element (Radiometer, model pHG201-8). The glass electrode was calibrated by the spectrophotometric method described by Kolthoff and Chantooni[20] using an Agilent 8453 spectrophotometer. The acid−base indicators employed were bromophenol blue (pK_a^{ACN} = 17.5), *p*-nitrophenol (pK_a^{ACN} = 20.7), and Phenol red (pK_a^{ACN} = 25.1).[21] The acid−base pair phenol/phenolate was used to modify the acidity level. The obtained slope for the *E* versus pH plot was 55 mV/dec The titrations were made using 0.1 M tetraethylammonium phenolate in CH$_3$-CN. The obtained values represent the average of five independent experiments. For the studied compounds, the homo-conjugation equilibrium constant was not considered in the analysis and is assumed to have a value of 10^2, as has been reported for 2-nitrophenol.[21]

Spectroelectrochemical ESR Measurements. ESR spectra were recorded, in the X band (9.85 GHz), using a Brucker ELEXSYS 500 instrument with a rectangular TE$_{102}$ cavity. A commercially available spectroelectrochemical cell (Wilmad) was used. A platinum mesh (≈0.2 cm^2) was introduced in the flat path of the cell and used as the working electrode. Another platinum wire was used as the counter electrode (2.5 cm^2). The Ag/0.01 mol L^{-1} AgNO$_3$ + 0.1 mol L^{-1} Bu$_4$NClO$_4$ reference in acetonitrile (BAS) was employed as the reference electrode. Potential sweep control was performed in a 100 B/W voltammetric analyzer of Bioanalytical Systems (BAS) with a personal computer interface. The employed solutions were prepared in the same fashion as the ones used for the electrochemical studies, performing IR compensation with *R* values determined from positive feedback measurements,[18] as implemented in the 100 B/W analyzer (25% overshooting was used).

ESR Simulations. PEST WinSim free software, version 0.96 (National Institute of Environmental Health Sciences), was used to perform ESR spectra simulation from the hyperfine coupling constant values (*a*) measured to compare with the experimental ones. This program was also useful to evaluate *a* values in the case when a direct measurement was difficult under the spectra acquisition conditions.

Theoretical Calculations. ZINDO/1 calculations,[22,23] were performed with HyperChem (HyperCube Inc.) version 7.51 to perform full geometry optimization (no geometry constrains) for the radical structures experimentally detected, employing UHF (unrestricted Hartree−Fock) calculations. Vibrational analysis was performed to check that the obtained structures were indeed the minimum-energy conformers, characterized by the lack of negative vibrational frequencies. These structures were used as inputs for single-point energy calculations. Single-point energy calculations were performed with the MP2/6-31G-(d,p) method[24] using the hybrid functional of Becke and Lee−Yang−Parr (B3LYP)[25] to account for electron correlation. From this data, spin density values were evaluated as the difference between α and β spin densities (from s-type orbitals in the case of H atoms and from the mean value obtained from p$_x$, p$_y$, and p$_z$ orbitals for N atoms) multiplied by the corresponding hyperfine coupling constant between the involved atom and the
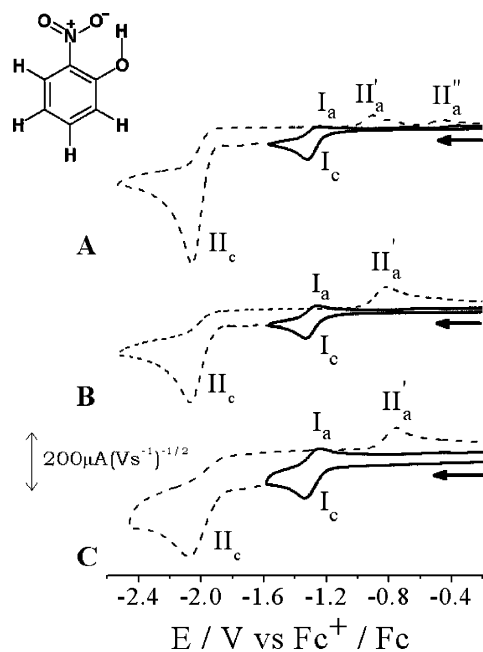
Figure 2. Cyclic voltammograms of 1.0 mM 2-nitrophenol (**1**) in CH$_3$-CN + 0.1 M Et$_4$NBF$_4$ on a glassy carbon electrode (0.07 cm^2). The potential scan was initiated from 0.4 V versus Fc$^+$/Fc (OCP) in the negative direction. The voltammetric responses were obtained at different scan potential rates, v (V s^{-1}): (A) 0.1; (B) 1; and (C) 8. Both reduction and oxidation peaks are indicated.

unpaired electron in the gas phase (506.9 G for H atoms and 549.5 G for N atoms[26]).

Results and Discussion

1. Electrochemical Study of 4-R-2-Nitrophenols. The typical cyclic voltammograms for 2-nitrophenol (**1**; R = −H) at different scan rates are shown in Figure 2.

From the voltammograms depicted, the presence of two reduction signals (I$_c$ and II$_c$) can be seen. By inverting the potential scan at values just above the potential of the first voltammetric peak (0.1 V s^{-1}, Figure 2A), the first peak shows an apparently irreversible behavior. However, by increasing the scan rate, an oxidation signal ($\Delta Ep_{Ic-Ia} \approx$ 0.06 V) can be detected, associated with the signal Ic (1 V s^{-1} Figure 2B and 8 V s^{-1}, Figure 2C). The peak current of this associated oxidation signal (Ip_{Ia}) increases with the scan rate, as occurs for a system in which coupled chemical reactions occur after the first electron-transfer process.[27] The second reduction signal, II$_c$, is associated with the presence of two oxidation signals (II$_a'$ and II$_a''$) at low scan rates (Figure 2A). When the scan rate increases, the oxidation current signal II$_a''$ diminishes until it disappears (Figure 2B and C). It is important to note that in most of the studies reported up to date, the voltammetric analysis is restricted to the potential window where the first reduction peak appears.[10,13,15]

The electrochemical behavior of **1** is followed in general terms for the whole family of studied 4-R-2-nitrophenols (Figures 3 and 4), as two main reduction processes are observable (peaks I$_c$ and II$_c$). However, for each compound, the electrochemical behavior changes with the scan rate. In the case of compound **1a** (−OCH$_3$ derivative, Figure 3), the first reduction process attains a reversible behavior upon inversion of the potential scan just after peak I$_c$ (Figure 3A) at lower scan rates than those where a similar behavior occurs for compound **1** (1 V s^{-1}, Figure 2B). This voltammetric behavior for the signal I$_c$ for compound **1b** (−CH$_3$ derivative) is similar to the one presented for
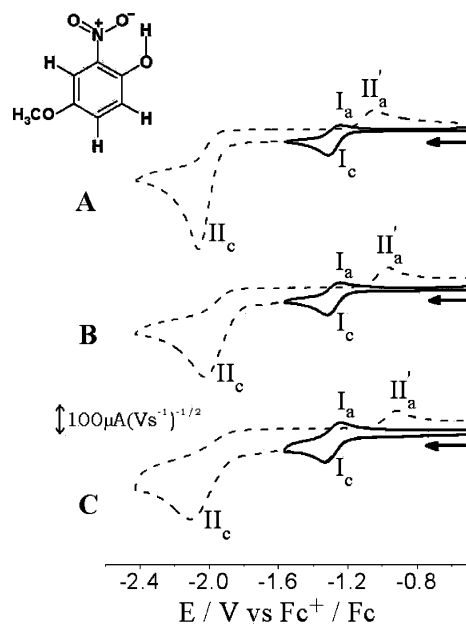

Figure 3. Cyclic voltammograms of 1.0 mM 4-methoxy-2-nitrophenol (**1a**) in CH$_3$CN + 0.1 M Et$_4$NBF$_4$ on a glassy carbon electrode (0.07 cm^2). The potential scan was initiated from −0.2 V versus Fc$^+$/Fc (OCP) in the negative direction. The voltammetric responses were obtained at different scan potential rates, v (V s^{-1}): (A) 0.1; (B) 1; and (C) 8. Both reduction and oxidation peaks are indicated.

Figure 4. Cyclic voltammograms of 1.0 mM 4-trifluoromethyl-2-nitrophenol (**1c**) in CH$_3$CN + 0.1 M Et$_4$NBF$_4$ on a glassy carbon electrode (0.07 cm^2). The potential scan was initiated from −0.2 V versus Fc$^+$/Fc (OCP) in the negative direction. The voltammetric responses were obtained at different scan potential rates, v (V s^{-1}): (A) 0.1; (B) 1; and (C) 8. Both reduction and oxidation peaks are indicated.
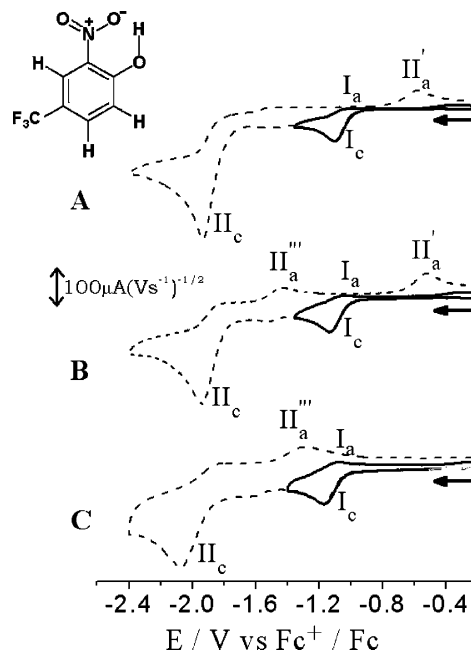
compound **1a**, which indicates that the reduction mechanism occurring at peak I$_c$ for compounds **1a** and **1b** is analogous.

Upon inversion of the potential scan after the reduction peak II$_c$, compounds **1a** and **1b** show only one oxidation signal (II$_a'$, Figure 3A), differing from the case of compound **1** at low scan rates, where two oxidation signals occur (Figure 2A). The reduction signal II$_c$ shows an irreversible behavior at the scan rates employed (Figure 3A−C).

The voltammetric behavior for the $-CF_3$ derivative (**1c**) is presented in Figure 4, which is similar to the behavior occurring for the $-CN$ derivative (**1d**). For compound **1c**, a reversible oxidation signal associated wit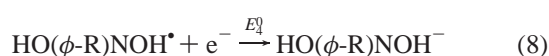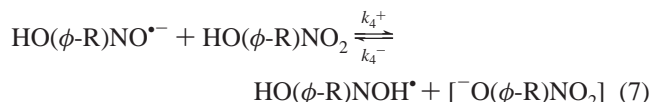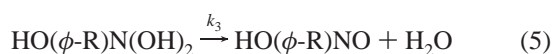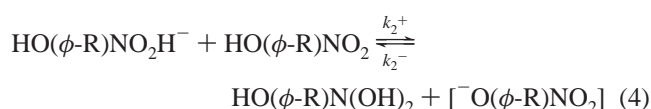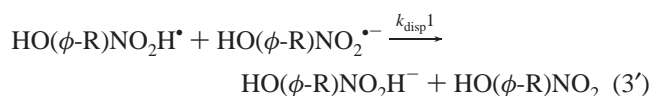h the reduction process I_c can be detected only upon employing high scan rates (approx. 10 V s^{-1}, Figure 4C), but the associated peak current (Ip_{Ia}) does not grow significantly. In the case of derivative **1d**, the reversible oxidation signal associated with peak I_c is detected at scan rates of 30 V s^{-1}. These results indicate that the mechanism involved in the electron uptake at compounds **1c** and **1d** is similar, but the rate of the process limiting the electrochemical pathway is different from the case presented above for derivatives **1a** and **1b**.

Upon inversion of the potential scan after the second reduction peak (II_c), compounds **1c** and **1d** show only one oxidation signal (II_a', Figure 4). This signal disappears upon the increase of the scan rate, but simultaneously, an oxidation signal begins to appear at scan rates higher than 1 V s^{-1} (II_a''', Figure 4B and C). The reduction signal II_c shows an irreversible behavior at the scan rates employed, in a similar way as occurred for compounds **1a** and **1b**.
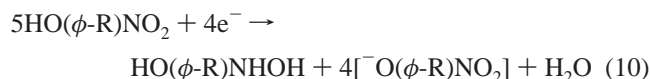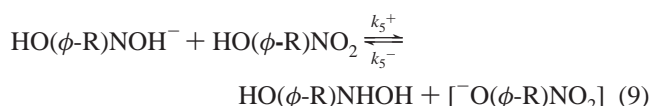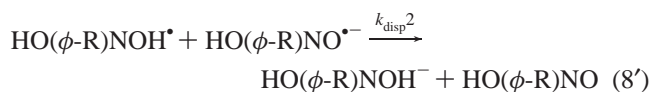
The voltammograms depicted in Figures 2−4 illustrate the complexity of the mechanisms involved in the electron transfer of the studied compounds and show also the influence of the inductive effect of the substituent on either the reactivity of the electrogenerated anions or the acidity of the phenolic function. In order to analyze these changes in terms of the properties of the substituents present, it is important to take into account the overall sequence occurring at the reduction signal Ic. The reduction pathway occurring at peak I_c for nitrophenols was proposed earlier by Amatore and co-workers[8] for the case where R = −H, as follows

$$HO(\phi\text{-R})NO_2 + e^- \xrightarrow{E_1^0} HO(\phi\text{-R})NO_2^{\bullet-} \quad (1)$$

$$HO(\phi\text{-R})NO_2^{\bullet-} + HO(\phi\text{-R})NO_2 \underset{k_1^-}{\overset{k_1^+}{\rightleftharpoons}}$$
$$HO(\phi\text{-R})NO_2H^{\bullet} + [^-O(\phi\text{-R})NO_2] \quad (2)$$

$$HO(\phi\text{-R})NO_2H^{\bullet} + e^- \xrightarrow{E_2^0} HO(\phi\text{-R})NO_2H^- \quad (3)$$

or

$$HO(\phi\text{-R})NO_2H^{\bullet} + HO(\phi\text{-R})NO_2^{\bullet-} \xrightarrow{k_{disp}1}$$
$$HO(\phi\text{-R})NO_2H^- + HO(\phi\text{-R})NO_2 \quad (3')$$

$$HO(\phi\text{-R})NO_2H^- + HO(\phi\text{-R})NO_2 \underset{k_2^-}{\overset{k_2^+}{\rightleftharpoons}}$$
$$HO(\phi\text{-R})N(OH)_2 + [^-O(\phi\text{-R})NO_2] \quad (4)$$

$$HO(\phi\text{-R})N(OH)_2 \xrightarrow{k_3} HO(\phi\text{-R})NO + H_2O \quad (5)$$

$$HO(\phi\text{-R})NO + e^- \xrightarrow{E_3^0} HO(\phi\text{-R})NO^{\bullet-} \quad (6)$$

$$HO(\phi\text{-R})NO^{\bullet-} + HO(\phi\text{-R})NO_2 \underset{k_4^-}{\overset{k_4^+}{\rightleftharpoons}}$$
$$HO(\phi\text{-R})NOH^{\bullet} + [^-O(\phi\text{-R})NO_2] \quad (7)$$

$$HO(\phi\text{-R})NOH^{\bullet} + e^- \xrightarrow{E_4^0} HO(\phi\text{-R})NOH^- \quad (8)$$

or

$$HO(\phi\text{-R})NOH^{\bullet} + HO(\phi\text{-R})NO^{\bullet-} \xrightarrow{k_{disp}2}$$
$$HO(\phi\text{-R})NOH^- + HO(\phi\text{-R})NO \quad (8')$$

$$HO(\phi\text{-R})NOH^- + HO(\phi\text{-R})NO_2 \underset{k_5^-}{\overset{k_5^+}{\rightleftharpoons}}$$
$$HO(\phi\text{-R})NHOH + [^-O(\phi\text{-R})NO_2] \quad (9)$$

$$5HO(\phi\text{-R})NO_2 + 4e^- \rightarrow$$
$$HO(\phi\text{-R})NHOH + 4[^-O(\phi\text{-R})NO_2] + H_2O \quad (10)$$

The global reaction occurring at peak I_c corresponds to the reaction presented as eq 10. The electronic stoichiometry at this reduction signal involves the consumption of 4/5 e$^-$ per mole of nitrophenol, where only 1/5 of nitrophenol is reduced into the hydroxylamine, while 4/5 mole of nitrophenols are deprotonated in the process. This type of process is known as a self-protonation pathway[8] since the original compound acts as the proton source during the upcoming protonation reactions (eq 2, 4, 7, or 9). On the basis of this mechanism, the electrogenerated products from the reduction of the studied compounds (Figure 1) are responsible for the further reduction (II_c) and oxidation signals observed (I_a, II_a', II_a''', Figures 2−4). The behavior of the signal Ia with the scan rate (increasing its intensity at higher scan rates) suggests that it is related to the oxidation of the first electrogenerated anion radical (eq 1), as the forthcoming self-protonation sequence is avoided by diminishing the time scale of the experiments. Therefore, the remaining anodic signals are related to the oxidation of the electrogenerated products during the overall sequence, such as the hydroxylamine (eq 9) or the phenolate anion (eq 2, 4, 7, or 9). As can be seen in Figures 2−4, the formation rate of these products is dependent on both the molecular structure and the time scale of the experiment performed. Therefore, it is more useful to evaluate the changes in the experimental behavior of the reduction signals of the studied compounds to obtain quantitative relationships, and the forthcoming discussion will be focused on this matter.

2. Analysis of the Reduction of 4-R-2-Nitrophenols to Hydroxylamine. At sufficiently high scan rates (between 1 and 30 V s^{-1}, Table 1), it was possible to evaluate the $E_{1/2}$ data as the average of the peak potential values of Ep_{Ic} and Ep_{Ia}. At such rates, the behavior of the electrochemical process is related only to the first electron uptake (eq 1), and therefore, the reduction process I_c is not effected by the self-protonation pathway. These values were correlated to the corresponding Hammett sigma parameter, σ_m[28] for the proper substituent −R in the *meta* position with respect to the nitro group (Figure 1). For the pair of signals I_c−I_a, this correlation showed that compound **1b**, which has an electron-donating inductive substituent effect (**1b**, $\sigma_m < 0$), has a peak potential value more negative than that of the 4-R-2-nitrophenols having an electron-withdrawing inductive effect (**1a**, **1c**, **1d**, $\sigma_m > 0$). The corresponding Hammett-Zuman-type[29] relationship $\Delta E_{1/2} = (E_{1/2})_x - (E_{1/2})_H$, where $(E_{1/2})_x$ is the $E_{1/2}$ value for a compound bearing a given substituent (x) and $(E_{1/2})_H$ is the value obtained from the compound bearing a proton (−H) as a substituent, presented a linear relationship with the σ_m values, leading to the linear equation $\Delta E_{1/2} = 0.405\sigma_m - 0.003$ ($R^2 = 0.9822$). It was found that for peak II_c, there is no correlation between the σ_m values and the E_{pIIc} data, probably due to the fact that, in the case of peak II_c, it was not possible to decouple the possible chemical processes associated with the electron uptake.

Self-Protonation Processes in 2-Nitrophenols

J. Phys. Chem. A, Vol. 111, No. 37, 2007 **8997**

TABLE 1: Voltammetric Data Obtained from the Analysis of the Studied 4-R-2-Nitrophenols

compound	R	$E_{1/2}I^a$/V	$Ep_{IIc}{}^b$/V	$k_1{}^{+c}$/M^{-1} s^{-1}	$\sigma_p{}^d$	$\sigma_m{}^d$	$pK_a{}^e$
1a	$-OCH_3$	-1.27	-2.06	$0.7-0.8$	-0.27	0.12	24.87 ± 0.09
1b	$-CH_3$	-1.31	-2.06	$1.0-1.2$	-0.17	-0.07	25.11 ± 0.08
1	$-H$	-1.29	-2.06	$1.2-1.7$	0.0	0.0	23.83 ± 0.32
1c	$-CF_3$	-1.09	-1.95	$5-5.5$	0.54	0.43	19.36 ± 0.14
1d	$-CN$	-1.05	-2.03	$15-20$	0.66	0.56	18.50 ± 0.20

$^a E_{1/2} = 1/2(Ep_{Ic} + Ep_{Ia})$ in V versus Fc$^+$/Fc at **1a**: $\nu = 4$ V s^{-1}; **1b**: $\nu = 4$ V s^{-1}; **1**: $\nu = 4$ V s^{-1}; **1c**: $\nu = 6$ V s^{-1}; **1d**: $\nu = 80$ V s^{-1}. ^{b} In V versus Fc$^+$/Fc at $\nu = 0.1$ V s^{-1}. ^{c} Obtained from the analysis of the variations of the peak potential Ep_{Ic} and current ratio Ip_{Ia}/Ip_{Ic} as a function of the scan rate (Figure 5A and B). ^{d} Taken from ref 28. ^{e} Experimentally determined pK_a values in the acetonitrile solution.

Despite the obtained correlation described above between $\Delta E_{1/2}$ and σ_m, the voltammetric behavior for each 4-R-2-nitrophenol (Figures 2−4) suggests changes in the stability of the electrogenerated intermediates during the charge-transfer process I_c. These changes are not directly related to the inductive effect as described by the σ_m parameter; for example, the voltammetric behavior of derivative **1a**, bearing the $-OCH_3$ substituent ($\sigma_m > 0$), has a similar voltammetric behavior to that of compound **1b** ($-CH_3$ derivative, $\sigma_m < 0$). Furthermore, the recovery in current for the process associated with the reoxidation of the anion radical electrogenerated from eq 1 (peak I_a) shows differences in terms of the analyzed compounds, as the scan rates required to observe this process are different for each compound. In order to understand how a particular substituent alters the reduction pathway for each compound, it is necessary to study the kinetics of the mechanism related to this voltammetric signal.

From the voltammograms presented above (Figures 2−4), the more noticeable effect observed is the decoupling of the self-protonation pathway (eqs 2−9) at higher scan rates, obtaining quasi-reversible voltammetric responses. In this type of complex schemes, the rate of the global process (eq 10) can be determined by one of the next steps: the rate of self-protonation of the anion radical ($k_1{}^+$, eq 2) and the competition between the transformation of the neutral radical into an anion by a heterogeneous electron transfer (eq 3) or by the rate of disproportionation between the neutral radical and the anion radical ($k_{disp}1$, eq 3′).[8,28] In the analysis of the responses obtained for systems presenting this competition, the analyzed signals vary only slightly in the region where the EC transition occurs since the presence of the reduction process occurring by eqs 3 or 3′ is favored due to the less negative potential value of the electron transfer occurring as eq 3.[30] However, the presented scheme appears to be even more complex, as the dehydration step previous to the formation of the nitroso derivative (k_3, eq 5) or the forthcoming protonation steps during the reduction of the nitroso derivative ($k_4{}^+$, $k_5{}^+$, eqs 7 and 9) could also be rate-determining steps. In the case of eq 6, it is known that the reduction of the nitroso derivative occurs typically at less negative potential values than the reduction of the nitro function.[31,32] The easier reduction of such an intermediate would therefore act as a driving force (along with the formation of water, which is a very stable molecule) for eq 5 to be shifted to the right of the reaction sequence. However, in the case of the remaining protonation steps (eqs 7 and 9), the basicity of the nitroso anion radical is expected to be a little lower than the one presented for the nitro anion radical, and they could act as rate-determining steps but at longer time scales due to the high requirements in the protonated 2-nitrophenol, which demands that the reaction layer considering these processes would be higher than that during the first half of the sequence (eqs 1−4).

It is interesting to note that the experimental voltammograms suggests that, by recovering the oxidation signal of the anion radical (I_a), there is a time scale in which the first protonation

step (eq 2) is likely to be the rate-determining step (RDS). With the purpose of obtaining an approximate value of such a rate (labeled as $k_1{}^+$), the overall mechanism, depicted by eqs 1−9, was simulated employing the program DigiElch version 3.0, considering such a step as the RDS and considering all other rates in the process to be very large ($k_2{}^+$, k_3, $k_4{}^+$, $k_5{}^+ = 10^4$). This type of simulation (considering the whole mechanism depicted in eqs 1−9) has not been considered in the literature, although the approximation that the first protonation step is the RDS was employed by Amatore and co-workers[8] to describe the reactivity of several systems where self-protonation mechanisms are involved. From these simulated voltammograms, the evaluation of the variations of the peak potential Ep_{Ic} and the current ratio Ip_{Ia}/Ip_{Ic} was determined as a function of the kinetic parameter $\lambda = k_1{}^+C^*RT/(\nu F)$, considering a second-order mechanism, which allowed construction of the respective theoretical curves representing the general behavior of the presented mechanism (continuous lines in Figures 5A and 5B). C^* is the bulk concentration of the studied nitrophenols at each plot. The experimental data were correspondingly fitted into each theoretical curve, obtaining estimated values of $k_1{}^+$ for each plot, both of them on the same order of magnitude (Table 1). It should be noticed that the experimental variations of the Ep_{Ic} and the current ratio Ip_{Ia}/Ip_{Ic} values present a fairly good fit with the simulated responses (Figure 5), suggesting that, at a given time scale ($-3 < \lambda < 1$), the assumption that the first protonation reaction (eq 2) is the RDS is a good approximation.

The obtained $k_1{}^+$ data (Table 1) do not show a linear correlation with the corresponding σ_m value. However, the relationship with the corresponding σ_p value of the given substituent[28] (Table 1) leads to a good relationship with the experimental data, obtaining the following linear relationship: $\log k_1{}^+ = 1.207\sigma_p - 0.227$ ($R^2 = 0.9741$). It should be noticed that a linear correlation appears also upon comparing the experimentally obtained $pK_a{}^{CH_3CN}$ values of the corresponding phenols in acetonitrile (Table 1) with the less acidic compounds (**1**, **1a**, and **1b**), presenting the lowest effect of the protonation reaction (lower $k_1{}^+$ values), while the opposite effect occurs for the most acidic 4-R-2-nitrophenols **1c** and **1d**. This result suggests that, even though the energetics of the reduction process is determined by the inductive effect of the substituent in the 4-position (*meta* with respect of the nitro group, Figure 1), the kinetics of the electrochemical mechanism will be determined by the rate of the first protonation step on which the acidity level of each phenol function is the determining factor associated with the inductive effect of the substituent in the 4-position (*para* with respect of the $-OH$ group, Figure 1). It should be noticed that the obtained $k_1{}^+$ values are about 2 orders of magnitude lower than the value reported in DMSO solution.[8] However, it has been reported that pK_a values of 2-nitrophenol are about 2 orders of magnitude lower in DMSO solution than those in CH$_3$-CN,[21] which indicates that the protonation reactions in CH$_3$CN should occur at a lower rate than in the former solvent, which would account for the observed difference.
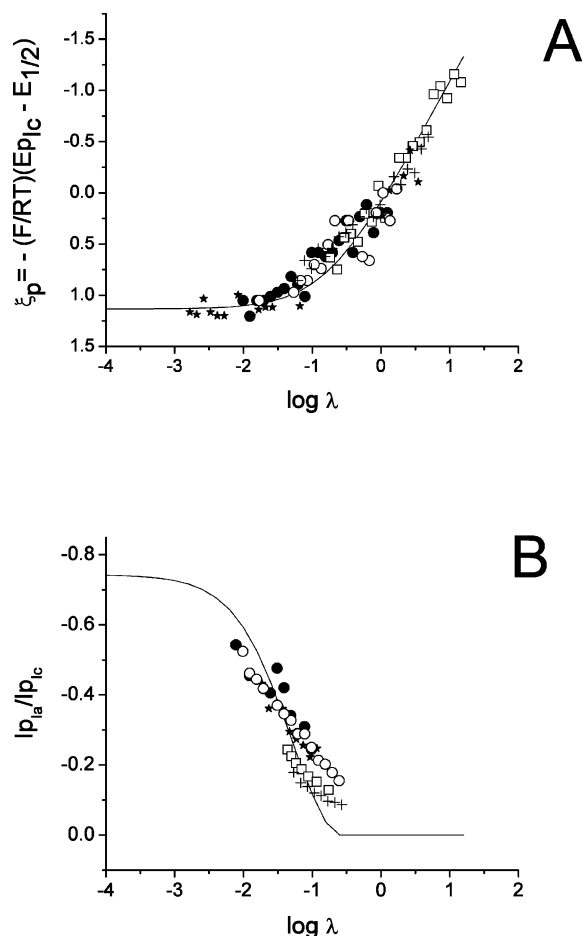
Figure 5. (A) Variation of the peak potential and (B) variation of the current ratio Ip_{Ic}/Ip_{Ia} for 2-nitrophenol **1** (★), 4-methoxy-2-nitrophenol **1a** (●), 4-methyl-2-nitrophenol **1b** (○), 3-trifluoro-2-nitrophenol **1c** (+), and 2-hydroxybenzonitrile **1d** (□) as a function of the kinetic parameter $\lambda = k_1^+ C^* RT/(vF)$. Continuous lines represent the theoretical variations for the estimated voltammetric peak parameters considering the mechanistic sequence depicted in eqs 1−9.

The above-presented results confirm that, despite the complexity involved during the electron- and proton-transfer pathways at potential peak I_c (eqs 1−10), it was possible to analyze the changes in stability of the first electrogenerated anion radical, which is directly influenced by the chemical structure of the studied 4-R-2-nitrophenols. These effects are related to the changes in the protonation rate of the corresponding anion radicals which are generated during the voltammetric experiments. The stability of the anion radicals will be considered further during the spectroelectrochemical ESR study. Yet, in order to complete the analysis of the electrochemical reduction processes for the studied compounds, the analysis of the voltammetric behavior of the second reduction II_c process was performed.

3. Analysis of the Second Reduction Process of 4-R-2-Nitrophenols. Considering the above-presented reaction pathway (eqs 1−9), the reduction process occurring at peak II_c should be related to the reduction of a product of the overall self-protonation sequence (eq 10). The species being reduced at this potential value was demonstrated to be the deprotonated 2-nitrophenolate anion [$^-$O(ϕ-R)NO$_2$], which emerges from each protonation step.[33] This was confirmed by performing experiments of a solution of compound **1** in the presence of an equivalent of a tetraethylammonium hydroxide (Figure 6B) and by reducing the chemically generated salt (tetraethylammonium 2-nitrophenolate, Figure 6C).
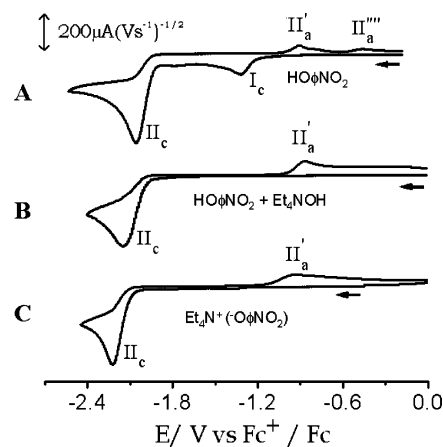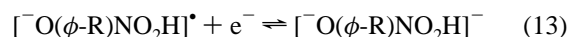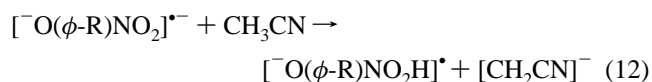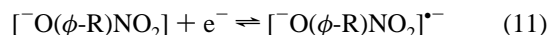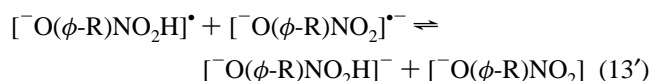

Figure 6. Cyclic voltammograms obtained in CH_3CN + 0.1 M Et_4-NBF_4 on a glassy carbon electrode (0.07 cm^2) in the presence of different compounds: (A) 1.0 mM 2-nitrophenol (**1**), (B) 1.0 mM 2-nitrophenol (**1**) with 1 equiv of tetrabutylammonium hydroxide, and (C) 1.0 mM tetraethylammonium 2-nitrophenolate. The potential scan was initiated from −0.2 V versus Fc$^+$/Fc (OCP) in the negative direction. $v = 0.1$ V s^{-1} is shown. Both reduction and oxidation peaks are indicated.

The voltammograms presented in Figure 6B and C show that the corresponding conjugated base of the 2-nitrophenol [$^-$O(ϕ-R)NO$_2$] is reduced at the same potential value as that of peak II_c for the neutral compound **1** (Figure 6A). The same behavior was obtained for derivatives **1a**−**1d**. It should be mentioned that, to the best of our knowledge, the reduction pathway occurring at this signal has not been described in detail in the literature. Due to the irreversible behavior of signal II_c, the reduction mechanism occurring at this potential value for the studied 4-R-2-nitrophenols could involve a similar pathway as the one presented above for the neutral compound

$$[^-\text{O}(\phi\text{-R})\text{NO}_2] + \text{e}^- \rightleftharpoons [^-\text{O}(\phi\text{-R})\text{NO}_2]^{\bullet-} \qquad (11)$$

$$[^-\text{O}(\phi\text{-R})\text{NO}_2]^{\bullet-} + \text{CH}_3\text{CN} \rightarrow$$
$$[^-\text{O}(\phi\text{-R})\text{NO}_2\text{H}]^\bullet + [\text{CH}_2\text{CN}]^- \quad (12)$$

$$[^-\text{O}(\phi\text{-R})\text{NO}_2\text{H}]^\bullet + \text{e}^- \rightleftharpoons [^-\text{O}(\phi\text{-R})\text{NO}_2\text{H}]^- \qquad (13)$$

or

$$[^-\text{O}(\phi\text{-R})\text{NO}_2\text{H}]^\bullet + [^-\text{O}(\phi\text{-R})\text{NO}_2]^{\bullet-} \rightleftharpoons$$
$$[^-\text{O}(\phi\text{-R})\text{NO}_2\text{H}]^- + [^-\text{O}(\phi\text{-R})\text{NO}_2] \quad (13')$$

From eq 13 or 13′, the reduction pathway can undergo further protonation/reduction steps. However, it is important to note that, in this case, the protonation of the electrogenerated dianion radical ([$^-$O(ϕ-R)NO$_2$]$^{\bullet-}$, eq 11) is promoted by the employed solvent (CH$_3$CN, eq 12). This proposal arises from the fact that, at potential values near Ep_{IIc}, the interface is depleted from molecules of the corresponding 4-R-2-nitrophenol [HO(ϕ-R)-NO$_2$], and the solvent is the only source of protons. For this reason, it was necessary to study the chemical structure of this radical species by a spectroscopic method.

4. Spectroelectrochemical Study of 4-R-2-Nitrophenols. In order to study the stability of the electrogenerated anion radicals of the corresponding 4-R-2-nitrophenols in solution, spectroelectrochemical ESR studies were performed by varying the applied potential in the region of peak I_c.
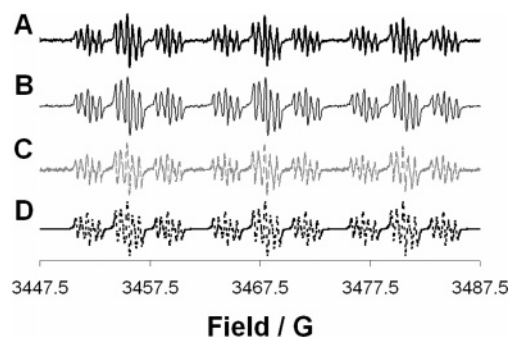
Self-Protonation Processes in 2-Nitrophenols

J. Phys. Chem. A, Vol. 111, No. 37, 2007 **8999**

Figure 7. ESR spectra of the chemical species formed by electrochemical reduction of a 2-nitrophenol-type (**1**) molecule at −2.1 V versus Fc$^+$/Fc in the presence of different experimental conditions: (A) 1 mM solution of **1**, (B) 1 mM solution of **1** + 1 equiv of tetraethylammonium hydroxide, and (C) 1 mM solution of tetraethylammonium 2-nitrophenolate. (D) Simulation of the ESR spectra presented with hyperfine coupling constant values determined experimentally (see Table 2).

At potential values just above peak I$_c$, no ESR signal was recorded, even though high accumulation times were employed (approx. 10 min). This result was obtained for all of the studied compounds and indicates that the nitro anion radical is not stable in solution. This demonstrates that, on the time scales of the spectroelectrochemical ESR experiments, the anion radical species electrogenerated at peak I$_c$ (eq 1) are not stable enough to afford a spin population high enough to be detectable. However, in previous studies performed in DMF or DMSO as the solvents,[33,34] the ESR signal proceeding from the nitro anion radical was detected and indicates again that the stability of the anion radical is strongly solvent-dependent, an issue which is not being further considered in this work.

It was reported earlier[35,36] that the dianion radical species electrogenerated from the one-electron reduction of deprotonated α-hydroxyquinones can be detected by ESR spectroelectrochemical measurements. Therefore, the spectroelectrochemical study was also performed at potential values near the peak II$_c$. At this region of the applied potential, ESR signals were detected for each compound, which was a surprising result as the peaks II$_c$ show an irreversible behavior (Figures 2−4).

In the case of derivative **1**, the ESR spectrum obtained experimentally at peak II$_c$ is presented in Figure 7A. The same spectral pattern was also obtained for the reduction of the deprotonated compound **1** both in the presence of 1 equiv of tetraethylammonium hydroxide (Figure 7B) and the reduction
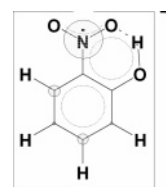

Figure 8. Spin density structure for the anion radical of 2-nitrophenol (**1**) evaluated from theoretical calculations at the B3LYP//6-31G(d,p) level (Table 2).

of the tetraethylammonium salt of 2-nitrophenolate (Figure 7C). This spectral structure was simulated (Figure 7D) employing five spin−proton hyperfine coupling constants (HFCC) and the corresponding HFCC value for the interaction between the unpaired electron and the N atom at position C-2 of the reduced nitro function (see Figure 1); the HFCC values used for the spectrum simulation are reported in Table 2.

The corresponding HFCC values were calculated at the B3LYP//6-31G(d,p) level (Table 2), showing a good correlation with the experimental data and thus confirming the presence of the anion radical structure at the applied potential value. The spin density contours based on the experimentally obtained HFCC values are presented in Figure 8.

The obtained result is interesting (Figure 7) since, at the experimental conditions of the voltammetric peak II$_c$, the species being reduced lacks a proton of the hydroxyl function at the position C-1 (eq 11) and should present only four HFCC values from proton−electron spin coupling. Therefore, this result indicates that the electrogenerated dianion radical (eq 11) is basic enough in CH$_3$CN to be protonated by the solvent (eq 12), generating the anion radical structure at more negative potential values than those observed for DMF or DMSO.[32,33] This was confirmed upon comparison of the corresponding HFCC values at each position with data previously reported in the literature.[33,34] However, the stability of this species proves to be low because, by switching off the applied potential, the anion radical decay rate is very fast ($t_{1/2} \approx 1$ min). This result implicates that the formation of such species occurs in a transient way in CH$_3$-CN. To our best knowledge, this behavior has not been considered in previous works with 2-nitrophenols. It also shows that the protonation of the electrogenerated dianion radical (eq 12) is a rate-determining step in the sequence associated with the reduction process II$_c$, in a similar fashion as that which occurred during the analysis of the first reduction process I$_c$ (see above).

TABLE 2: Experimental Hyperfine Coupling Constant Values Obtained from the ESR Spectra of the Radical Species Detected during Spectroelectrochemical ESR Experiments in Et$_4$NBF$_4$/CH$_3$CN^a

compound	a_N/G	a_{H-3}/G	a_{H-4}/G	a_{H-5}/G	a_{H-6}/G	a-CX$_3$/G	a_{OH}/G	g
1a	11.98	4.01	NA	3.34	0.65	NA	0.48	2.0046
	(9.82)	(3.78)		(3.22)	(0.26)		(0.78)	
1b	12.42	3.77	NA	3.54	0.67	1.01	0.47	2.0046
	(10.09)	(4.00)		(3.43)	(0.03)	(0.56)^c	(0.6)	
1	12.52	3.69	1.04	3.6	0.65	NA	0.45	2.0044
	(10.15)	(3.91)	(1.45)	(3.56)	(0.08)		(0.80)	
1c	14.02	2.32	NA	3.43	ND	ND	ND	2.0044
	(8.80)	(3.46)		(4.92)	(0.08)		(1.00)	
1d	13.4	2.02	NA	3.88	0.4	NA	ND	2.0043
	(6.19)	(3.14)		(5.25)	(0.16)		(1.00)	
1a^b	11.90	4.01	NA	3.34	0.65	NA	ND	2.0045
	(9.83)	(3.78)		(3.22)	(0.26)			
1^b	12.39	3.67	1.06	3.66	0.68	NA	ND	2.0046
	(10.5)	(3.91)	(1.45)	(3.56)	(0.08)			

^{a} See Figure 1 for position numbering. NA: Not applicable; ND: Not detected. Data in parentheses represent the calculated spin density employing the B3LYP//6-31G(d,p) method for an anion radical structure. ^{b} Data obtained in an Et$_4$NBF$_4$/CD$_3$CN solution. ^{c} X=H corresponds to a quartet splitting of the signal by the CH$_3$ group.
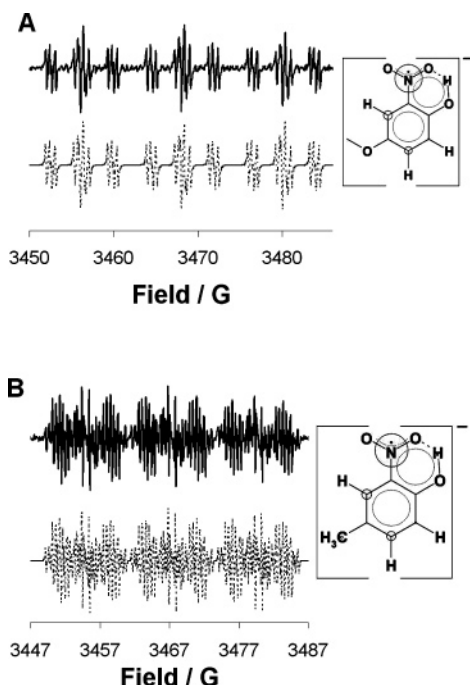
Figure 9. ESR spectra of the electrogenerated radical species, at −2.2 V vs Fc$^+$/Fc, of 1 mM solutions in an Et$_4$NBF$_4$/CH$_3$CN solution of (A) 4-OCH$_3$-2-nitrophenol (**1a**) and (B) 4-CH$_3$-2-nitrophenol (**1b**). The upper solid line represents the experimental spectrum, while the dotted lower line shows the simulated response.
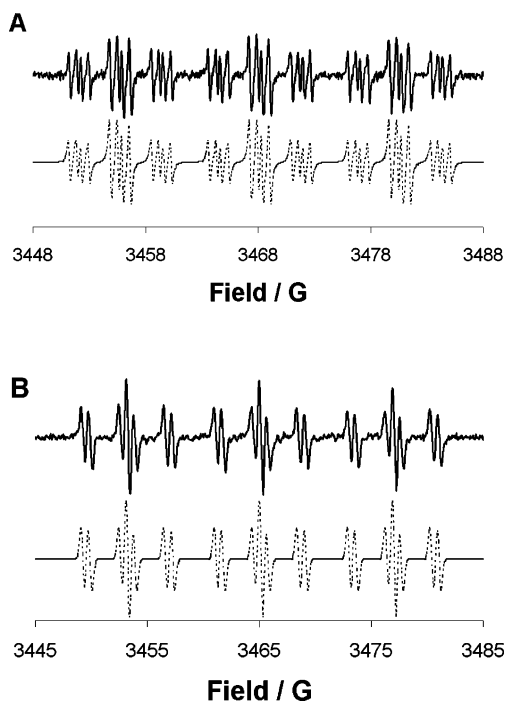

Figure 10. ESR spectra of the electrogenerated radical species, at −2.2 V versus Fc$^+$/Fc, in an Et$_4$NBF$_4$/CD$_3$CN solution of 1 mM solutions of (A) 2-nitrophenol (**1**) and (B) 4-OCH$_3$-2-nitrophenol (**1a**). The upper solid line represents the experimental spectrum, while the dotted lower line shows the simulated response.

For the remaining compounds, different spectral structures were obtained by applying potential values in the region of the voltammetric peak II$_c$ (Figures 9−11). However, the spin-coupling hyperfine structures revealed differences in the chemical nature of the electrogenerated radical. In the case of the −OCH$_3$ derivative **1a**, an anion radical structure was obtained (Figure 9A), characterized by the presence of four proton-spin
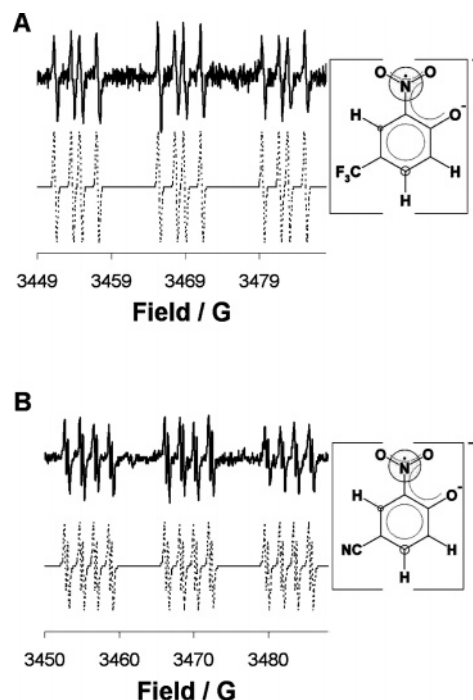

Figure 11. ESR spectra of the electrogenerated radical species, at −2.2 V versus Fc$^+$/Fc, of 1 mM solutions of (A) 4-CF$_3$-nitrophenol (**1c**) and (B) 4-CN-2-nitrophenol (**1d**) in Et$_4$NBF$_4$/CH$_3$CN. The upper solid line represents the experimental spectrum, while the dotted lower line shows the simulated response. The spin density structure evaluated from the analysis of the experimental data is shown in the Figure.

HFCC values, associated with coupling with the proton atoms at positions C-3, C-5, and C-6 and that at the hydroxyl group at C-1, along with the corresponding HFCC for the interaction between the unpaired electron and the N atom at position C-2 (Table 2). The electrogenerated radical species from the −CH$_3$-substituted 2-nitrophenol **1b** shows a spectral pattern upon reduction at peak II$_c$, consisting of six HFCC values (Figure 9B, Table 2), one of them appearing as a quartet signal related to the coupling with the hydrogen atoms at the −CH$_3$ group, another with the N atom at position C-2 (of the reduced nitro group), and the rest associated with coupling with the protons at positions C-3, C-5, and C-6 and with the H atom of the hydroxyl function at C-1. The presented patterns show that, as in the case of **1**, for both compounds **1a** and **1b**, the dianion radical electrogenerated at these potential values protonates readily to form the corresponding anion radical. Once again, the calculated HFCC values at the B3LYP//6-31G(d,p) level for these anion radical structures (Table 2) are fairly related to the experimentally obtained data and therefore confirm the presence of these species.

The effect of the solvent protonation proposed above was confirmed by obtaining the corresponding ESR spectra of derivatives **1** and **1a** in CD$_3$CN (Figure 10A and B). The choice of the latter derivative was justified as it lacks the presence of the CH$_3$ group, which can generate a more complicated spectral pattern. The obtained spectra of both radical structures lack one HFCC value, in comparison with the spectra obtained in CH$_3$-CN (Figures 7A and 9A, Table 2). These missing HFCC values are associated with the lowest values for the corresponding anion radicals structures, related to the coupling of the unpaired electron and the hydroxyl function at C-1.

In the case of the compounds **1c** and **1d**, which bear the electron-withdrawing substituents −CF$_3$ and −CN, respectively, the obtained spectral patterns revealed a different nature in the electrogenerated anion radical structure (Figure 11A and B). In
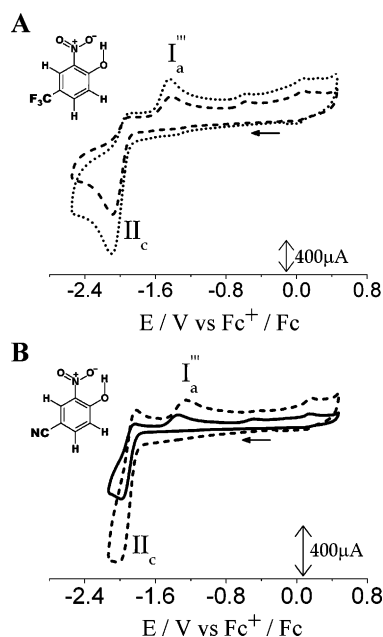
Self-Protonation Processes in 2-Nitrophenols

J. Phys. Chem. A, Vol. 111, No. 37, 2007 **9001**

Figure 12. Cyclic voltammograms obtained in CH_3CN + 0.1 M Et_4-NBF_4 on a glassy carbon electrode (0.07 cm^2) in the presence of (A) a 2.0 mM solution of 4-CF_3-nitrophenol (**1c**) + 2 equiv of tetraethylammonium hydroxide and (B) a 2.0 mM solution of 4-CN-2-nitrophenol (**1d**) with 2 equiv of tetraethylammonium hydroxide. The potential scan was initiated from −0.2 V versus Fc$^+$/Fc (OCP) in the negative direction. The voltammetric responses were obtained at different scan potential rates, v: 1 V s^{-1} (—), 5 V s^{-1} (- - -), and 10V s^{-1} (· · ·).

the case of the −CF_3-substituted 2-nitrophenol (**1c**), the ESR spectrum (Figure 10A) only showed the presence of two HFCC values, associated with coupling between the unpaired electron spin and protons at positions C-3 and C-5 and the corresponding HFCC value associated to coupling with the N atom at C-2 (Table 2). It is interesting to note that the spectral structure did not show hyperfine coupling between the unpaired electron spin and the F atoms, which indicates that the spin density is not high at the site near the −CF_3 substituent. For compound **1d**, the spectral structure indicates the presence of three HFCC values associated with coupling between the unpaired electron and the proton atoms at positions C-3, C-5, and C-6 in the chemical structure of the radical species and one HFCC value with the N atom at position C-2 (Figure 10B, Table 2).

The lack of ESR signals suggests that the structure being detected corresponds to a dianion radical species. This result was confirmed by calculating the HFCC values for each position of the molecule employing the B3LYP//6-31G(d,p) method, which leads to HFCC values associated with coupling between the unpaired electron and the N-2 atom lower than the experimental data (Table 2). This indicates that the spin density in the experimental case is higher than the one predicted by the employed method, thus revealing the presence of a species bearing a more negative charge, consistent with a dianion radical structure. It should be noticed that a quasi-reversible behavior for the reduction signal II_c was obtained only for the −CN derivative (**1d**, Figure 12) at scan rates higher than 5 V s^{-1}, which supports the formation of a stable radical dianion structure. Surprisingly, in the case of the −CF_3 compound, a partial reversibility pattern was not found in scan rates up to 10 V s^{-1}. However, the ESR results obtained for this compound (Figure 11) proved to be consistent with the formation of a dianion radical species.

The presented results indicate that the presence of the groups −OCH_3 and −CH_3 increases the basicity of the electrogenerated

dianion radical structure in front of the acidity of acetonitrile (eq 11) and that the detected intermediate is the protonated species generated during eq 12. This structure can be stabilized by the formation of an intramolecular hydrogen bond, as has been suggested during the study of the anion radical of 2-nitrophenol **1**.[8,32]

On the other hand, the presence of the −CN and −CF_3 groups at position C-4 diminishes the basicity of the dianion radical enough to avoid its protonation and confirms that the radical structures obtained during the electrochemical reduction of the studied 4-R-2-nitrophenol derivatives proceed through the formation of a dianion radical. Therefore, the substituents −OCH_3 and −CH_3 act as electron-donating groups, while −CF_3 and −CN behave as electron-withdrawing functions in front of the electrogenerated dianion radical structure, in a similar fashion as the behavior presented during the analysis of the reactivity of the first electrogenerated anion radicals (see section 2).

These "pure inductive" effects show an interesting result in terms of the HFCC values of the N atom at position C-2 (a_N, Table 2), which indicates an increase of the spin density at that position by increasing the electron-withdrawing character of the substituent (except for the −CN-substituted compound; see below), considering the validity of the McConnell relationship.[37,38]

$$a_H = Q\rho \qquad (14)$$

This effect occurs even though two different types of radical species are being electrogenerated for electron-donating (anion radicals) and electron-withdrawing substituted 2-nitrophenols (dianion radicals). This result is exactly opposed to the case of the anion radicals electrogenerated from substituted nitrobenzenes[39] and implies that changes in the chemical nature of the electrogenerated anion radical are reflected in the variations of the experimental spin density of the N atom at position C-2 for different kinds of electrogenerated species. However, the pure inductive effect of the substituent can be indeed detected in the case of the HFCC values at position H-3 (between the reduced nitro function and the substituent), where it follows the expected relationship.

Another interesting result is related to the spin density at the site C-6 ($a_{H−6}$, Table 2). This site shows that, in the case of the dianion radical of **1c** (−CF_3 substituent), this position has a very low value of spin density, as a HFCC value is not experimentally detected. However, this position shows a HFCC value in the case of the −CN-substituted radical species ($a_{H−6}$, Table 2). It should be noticed that the HFCC value of the N atom (a_N, Table 2) in the latter case is lower than that in the case of the −CF_3-substituted compound, which suggests that the −CN substituent has a certain resonant character, which lowers the spin density at N-2 and distributes the spin density in the radical species more effectively than −CF_3.

Conclusions

A voltammetric and spectroelectrochemical ESR study of the reduction processes of five substituted 4-R-2-nitrophenols (R = −H, −OCH_3, −CH_3, −CN, and −CF_3) in acetonitrile was performed. In the potential range here considered (−0.2 to −2.5 V vs Fc$^+$/Fc), two reduction signals (I_c and II_c) were detected; the first one was associated with the formation of the corresponding hydroxylamine via a self-protonation mechanism. The voltammetric analysis at the first reduction signal showed that there are differences in the reduction pathway for each substituted 4-R-2-nitrophenol, being the $E_{1/2}$ values determined

by the inductive effect of the substituent in the *meta* position with respect of the nitro group leading to a linear Hammett-Zuman relationship $\Delta E_{1/2} = 0.405\sigma_m - 0.003$ ($R^2 = 0.9822$), while the electron-transfer kinetics was determined by the rate of the protonation (k_1^+) of the electrogenerated anion radical, directly related to the influence of the substituent in the *para* position with respect to the $-OH$ moiety, $\log k_1^+ = 1.207\sigma_p - 0.227$ ($R^2 = 0.9741$). However, at potential values near the first reduction peak, no ESR signal was recorded, indicating the instability of the radical species in solution. Nevertheless, an intense ESR spectra generated at the second reduction peak was detected for all compounds, indicating the monoelectronic reduction of the corresponding deprotonated 4-R-2-nitrophenols. The spin-coupling hyperfine structures revealed differences in the chemical nature of the electrogenerated radical; meanwhile, the $-CF_3$ and $-CN$ substituents induced the formation of a dianion radical structure, and the $-H$, $-CH_3$, and $-OCH_3$ substituents provoked the formation of an anion radical structure due to the protonation by acetonitrile molecules of the initially electrogenerated dianion radical. This behavior was confirmed by analyzing the ESR spectra in deuterated acetonitrile and by performing quantum chemical calculations of the spin densities at each site of the electrogenerated anionic radicals.

References and Notes

(1) Abreu, F. C.; Tonholo, J.; Bottecchia, O.; Zani, C. L.; Goulart, M. O. F. *J. Electroanal. Chem.* **1999**, *462*, 195.

(2) Li, Q. X.; Zhao, J. M. S.; Gee, S. J.; Kurth, M. J.; Seiber, J. N.; Hammock, B. D. *J. Agric. Food Chem.* **1991**, *39*, 1885.

(3) Chopineaux-Courtois, V.; Reymond, F.; Bouchard, G.; Carrupt, P. A.; Testa, B.; Girault, H. H. *J. Am. Chem. Soc.* **1999**, *121*, 1743.

(4) Nivinskas, H.; Koder, R. L.; Anusevièius, I.; Šarlauskas, J.; Miller, A. F.; Èenas, N. *Acta Biochim. Pol.* **2000**, *47*, 941.

(5) She, Z.; Gao, M.; Jin, Ch.; Chen, Y.; Yu, J. *Process Biochem.* **2005**, *40*, 3017.

(6) Blanchard-Fillion, B.; Prou, D.; Polydoro, M.; Spielberg, D.; Tsika, E.; Wang, Z.; Hazen, S. L.; Koval, M.; Przedborski, S.; Ischiropoulos, H. *J. Neurosci.* **2006**, *26*, 6124.

(7) Özkan, S. A.; Özkan, Y.; Sentürk, K. *J. Pharm. Biomed. Anal.* **1998**, *17*, 299.

(8) Amatore, C.; Capobianco, G.; Farnia, G.; Sandoná, G.; Saveant, J. M.; Severin, M. G.; Vianello, E. *J. Am. Chem. Soc.* **1985**, *107*, 1815.

(9) Piette, L. H.; Ludwig, P.; Adams, R. N. *J. Am. Chem. Soc.* **1962**, *84*, 4212.

(10) Bautista-Martínez, J. A.; González, I.; Aguilar-Martínez, M. *J. Electroanal. Chem.* **2004**, *573*, 289.

(11) Aguilar-Martínez, M.; Bautista-Martínez, J. A.; Macias-Ruvalcaba, N. A.; González, I.; Tovar, E.; Martin del Alizal, T.; Collera, O.; Cuevas, G. *J. Org. Chem.* **2001**, *66*, 8349.

(12) Bautista-Martínez, J. A.; González, I.; Aguilar-Martínez, M. *Electrochim. Acta* **2004**, *49*, 3403.

(13) Bontá, M.; Chauviere, G.; Périé, J.; Núñez-Vergara, L. J.; Squella, J. A. *Electrochim. Acta* **2002**, *47*, 4045.

(14) Hromadová, M.; Mořkovská, P.; Pospíšil, L.; Giannarelli, S. *J. Electroanal. Chem.* **2005**, *582*, 156.

(15) de Paula, F. S.; Sales, É. M.; Vallaro, M.; Frutero, R.; Goulart, M. O. F. *J. Electroanal. Chem.* **2005**, *579*, 33.

(16) Kraiya, Ch.; Singh, P.; Evans, D. H. *J. Electroanal. Chem.* **2004**, *563*, 203.

(17) Roe, D. K. Overcoming Solution Resistance with Stability and Grace in Potentiostatic Circuits. In *Laboratory Techniques in Electroanalytical Chemistry*; Kissinger, P. T., Heineman, W. R., Eds.; Marcel Dekker, Inc: New York, 1996.

(18) He, P.; Faulkner, L. R. *Anal. Chem.* **1986**, *58*, 517.

(19) Gritzner, G.; Küta, J. *Pure Appl. Chem.* **1984**, *4*, 462.

(20) Kolthoff, I. M.; Chantooni, M. K. *J. Am. Chem Soc.* **1965**, *87*, 4428.

(21) Izutsu, K. *Acid−Base Dissociation Constants in Dipolar Aprotic Solvents*; Blackwell Scientific Publications: Oxford, U.K., 1990.

(22) Head, J. D.; Zerner, M. C. *Chem. Phys. Lett.* **1985**, *122*, 264.

(23) Head, J. D.; Zerner, M. C. *Chem. Phys. Lett.* **1986**, *131*, 359.

(24) Hehre, W. J.; Ditchfield, R.; Pople, J. A. *J. Chem. Phys.* **1972**, *56*, 2257.

(25) Becke, A. D. *J. Chem. Phys.* **1993**, *98*, 5648.

(26) Wertz, J. E.; Bolton, J. R. *Electron Spin Resonance*, 1st ed.; Chapman and Hall: New York, 1972.

(27) Savéant, J. M. *Elements of Molecular and Biomolecular Electrochemistry*; Wiley-Interscience: Hoboken, NJ, 2006.

(28) Hansch, C.; Leo, A.; Taft, R. W. *Chem. Rev.* **1991**, *91*, 185.

(29) Zuman, P. *Substituent Effects in Organic Polarography*; Plenum Press: New York, 1967.

(30) Amatore, C.; Savéant, J. M. *J. Electroanal. Chem.* **1977**, *85*, 27.

(31) Fialho-Oliveira, M. C. *Electrochim. Acta* **2003**, *48*, 1829.

(32) Silvester, D. S.; Wain, A. J.; Aldous, L.; Hardacre, C.; Compton, R. G. *J. Electroanal. Chem.* **2006**, *596*, 131.

(33) Farnia, G.; da Silva, A. R.; Vianello, E. *J. Electroanal. Chem.* **1974**, *57*, 191.

(34) Nordio, P. L.; Pavan, M. V.; Corvaja, C. *Trans. Faraday Soc.* **1964**, *60*, 1985.

(35) Frontana, C.; Frontana-Uribe, B. A.; González, I. *J. Electroanal. Chem.* **2004**, *573*, 307.

(36) Frontana, C.; González, I. *J. Electroanal. Chem.* **2007**, *603*, 155.

(37) McConnell, H. M. *J. Chem. Phys.* **1956**, *24*, 756.

(38) McConnell, H. M.; Chesnut, D. B. *J. Chem. Phys.* **1958**, *28*, 107.

(39) Maki, A. H.; Geske, D. H. *J. Am. Chem. Soc.* **1961**, *83*, 1852.